

Coupled-channels analysis of proton inelastic scattering to the γ -vibrational band in ^{24}Mg

L. Ray

Theoretical Division, Los Alamos Scientific Laboratory, Los Alamos, New Mexico 87545

G. S. Blanpied

Department of Physics, New Mexico State University, Las Cruces, New Mexico 88003

W. R. Coker

Department of Physics, University of Texas at Austin, Austin, Texas 78712

(Received 22 May 1979)

Results are presented of coupled-channels analyses of proton inelastic scattering data for the nucleus ^{24}Mg , in which the 2_2^+ , 4.24 MeV, 3^+ , 5.2 MeV, 4_2^+ , 6.01 MeV, and 5^+ (?), 7.8 MeV states of the γ -vibrational band are excited, at incident proton energies of 20.3, 40, and 800 MeV. Previous coupled-channels analyses of proton and α particle inelastic scattering data for these states in ^{24}Mg have completely failed to account for the shapes and magnitudes of the 3^+ , 4_2^+ , and 5^+ inelastic cross sections. In the present analysis, the inclusion of an additional nuclear vibrational multipole which permits a direct transition from the ground state to the 4_2^+ , 6.01 MeV state is shown to provide a tremendous improvement in the theoretical description of the inelastic cross sections of all the members of the γ -vibrational band, at each of the three incident proton energies considered. The same nuclear structure parameters are used at all three incident energies, along with phenomenological optical potentials specific to each energy. The new results for the 3^+ , 5.2 MeV state also shed light on the energy dependence of the direct spin-flip mechanism in proton inelastic scattering.

[NUCLEAR REACTIONS $^{24}\text{Mg}(p, p')$, $E_p=20.3, 40, \text{ and } 800 \text{ MeV}$; coupled-channels analysis; deformed-vibrational model; coupling parameters.]

I. INTRODUCTION

Vibrational states in deformed nuclei have attracted considerable attention from nuclear physicists for many years, with a number of studies of various kinds having been made in the s - d shell and in the rare earth and actinide regions.¹⁻¹³ In the even-even deformed nuclei, for instance, the first several excited states can be classified as belonging either to the ground state rotational band, or to the β - and γ -vibrational band sequences.^{1,14} Generally, these excited states have been investigated through the inelastic scattering of either protons²⁻⁷ or α particles⁸⁻¹¹ from the nuclei of interest. In the majority of these investigations, an effort was made to describe the inelastic scattering data in terms of macroscopic collective models of deformed nuclei¹⁴ and a coupled-channels reaction theory formalism, as developed, for example, by Tamura.¹⁵

For the specific case of ^{24}Mg , a number of analyses have been made of inelastic scattering data, employing the collective rotational model and the coupled-channels formalism.^{2-8,10} While these analyses have met with considerable success, there have also been significant failures. Calculated angular distributions for the 2^+ , 1.37 MeV and the 4^+ , 4.12 MeV members of the ground state

rotational band, as well as the 2_2^+ , 4.24 MeV "band-head" of the γ -vibrational band in ^{24}Mg , agree quite well in shape and magnitude with the measured cross sections and confirm the applicability of the simple rotational model to this nucleus. On the other hand, very drastic disagreement between predictions and data is found for the 8.12 MeV 6^+ state, assumed a member of the ground state rotational band, as well as for the 5.2 MeV 3^+ , the 6.01 MeV 4_2^+ , and the 7.8 MeV 5^+ states, assumed to be members of the γ -vibrational band.^{2-8,10} In this paper we will be particularly concerned with these latter discrepancies and their extirpation. The 7.8 MeV state is not definitely known to be a 5^+ (Ref. 16) but, following Blanpied *et al.*,² it will be assumed to be in what follows.

The nature of the failure of previous coupled-channels predictions^{2-8,10} for the angular distributions of the 3^+ , 4_2^+ , and 5^+ members of the γ -vibrational band of ^{24}Mg can be summarized as follows: Magnitude predictions are too small by one or two orders of magnitude, and the predicted shapes bear little resemblance to the data, often having slopes of the wrong algebraic sign. The drastic failure to predict the observed strength of the inelastic cross sections is common to both proton and α particle inelastic scattering^{8,10} and is not affected by inclusion or exclusion of spin-flip

processes for the protons.⁷ Coupling to other vibrational bands¹ also has no significant effect on the overall discrepancy.

However, if one has recourse to a spherically symmetric description of ²⁴Mg and the ordinary one-step distorted wave Born approximation (DWBA)¹⁷ one can obtain a good fit to the inelastic scattering data for the 6.01 MeV 4₂⁺ state.^{2,6,7,11} At 800 MeV, for instance, the DWBA fit to the 4₂⁺ state is good at forward angles, although it becomes out of phase with the data at the back angles.² This fact supplies the clue to what may be wrong with the coupled-channels calculations. Previous descriptions of the intrinsic nuclear vibrations about a deformed equilibrium shape have been restricted in such a way as to rule out a direct transition from the ground state to the 4₂⁺ state, by allowing (in the notation of Bohr¹⁴) only (Y'₂₂ + Y'₂₋₂) vibrations. Naqib and Blair¹¹ have previously argued that there exists a large Δl = 4 as well as Δl = 2 transition strength in ²⁴Mg, based on a particle-hole description of the 4₂⁺ state. The simplest way to take into account direct Δl = 4 paths is to include in the coupling potential such terms as (Y'₄₂ + Y'₄₋₂) (see Sec. II).

In the present work, we present new results of coupled-channels calculations for the ground and γ-vibrational bands in ²⁴Mg, excited by inelastic scattering of protons at 20.3,⁷ 40,⁶ and 800 (Ref. 2) MeV, paying particular attention to the effect of a direct transition from the ground state to the 4₂⁺ state on all of the coupled-channels predictions at these three energies, where rather complete data are available, particularly at 800 MeV.

The necessary extension of the deformed-vibrational nuclear collective model and the coupled-channels formalism is given in Sec. II. The results of the calculations and some conclusions are presented in Secs. III and IV, respectively.

II. EXTENSION OF THE DEFORMED-VIBRATIONAL MODEL

In this section the coupled-channels formalism of Tamura^{8,15} is extended to allow a direct coupling of the ground state and the 4₂⁺ state in the γ-vibrational band. The formulation given here assumes an even-even target nucleus. The deformed optical potential is taken to be of the form^{15,18}

$$V(r, \theta', \phi') = -V(1 + e_\nu)^{-1} - iW(1 + e_w)^{-1} - 4iW_{SF}e_{WSF}(1 + e_{WSF})^{-2} + V_{so}(r) + V_{Coul}(r), \quad (1)$$

where

$$e_i = \exp\{[r - R_i(\theta', \phi')]/a_i\} \quad (2)$$

and

$$R_i(\theta', \phi') = R_i \left[1 + \alpha_{20} Y'_{20} + \alpha_{40} Y'_{40} + \alpha_{22} (Y'_{22} + Y'_{2-2}) + \alpha_{42} (Y'_{42} + Y'_{4-2}) \right], \quad (3)$$

with $i = V, W,$ and WSF . The primes refer to the body-fixed coordinate system in which the Z' axis lies along the symmetry axis of the deformed intrinsic potential, and $V_{so}(r)$ and $V_{Coul}(r)$ are the usual spin-orbit and Coulomb potentials given explicitly in Refs. 15 and 18, taken here to be spherically symmetric. Hence, deformed spin-orbit¹⁹ and Coulomb excitation effects are neglected in our calculations. In addition, spin-flip processes which proceed via the spin-spin and tensor terms in the general proton-nucleus interaction potential will also be neglected. As in the work of Bohr,¹⁴ one can replace the quantities α_{20} and α_{22} with $\beta \cos \gamma$ and $(\beta/\sqrt{2}) \sin \gamma$, respectively. No such change of variables will be performed for the α_{40} and α_{42} parameters. An α_{44} term is omitted in Eq. (3) since no $K^\pi = 4^+$ vibrational band is considered here.¹

In general the nuclear radius parameter can be expanded as¹⁴

$$R_i(\theta', \phi') = R_i \left[1 + \sum_{\lambda\mu} \alpha_{\lambda\mu} Y_{\lambda\mu}(\theta', \phi') \right]. \quad (4)$$

The specific truncation of this expansion given in Eq. (3) is justified by the decreasing effect which the larger multipoles in the series in Eq. (4) have on the low-lying states and the limitation of our analysis to the ground ($K^\pi = 0^+$) and the γ bands ($K^\pi = 2^-$). The new feature of the multipole expansion included here is the addition of the $\alpha_{42}(Y'_{42} + Y'_{4-2})$ term in Eq. (3). Rush and Ganguly³ assumed Eq. (3) with $\alpha_{42} = 0$, and varied the $\alpha_{40} Y'_{40}$ term in order to fit the 6.01 MeV 4₂⁺ state, thus grossly overestimating the 4.12 MeV 4₁⁺ state. Clearly Eq. (3) is a more satisfactory generalization than that adopted in Ref. 3. Equation (3) allows the 4⁺ states at 4.12 and 6.01 MeV to be included simultaneously in a consistent way.

Expanding the potential to first order in α_{22} and α_{42} yields^{8,15}

$$V(r, \theta', \phi') \simeq V_1(r, \theta') + \alpha_{22} V_2(r, \theta') (Y'_{22} + Y'_{2-2}) + \alpha_{42} V_2(r, \theta') (Y'_{42} + Y'_{4-2}) + V_{so}(r) + V_{Coul}(r), \quad (5)$$

where $V_1(r, \theta')$ is obtained from the first three terms of Eq. (1), using Eqs. (2) and (3) with $\alpha_{22} = \alpha_{42} = 0$. The potential $V_2(r, \theta')$ is given by

$$V_2(r, \theta') = \left[-V(R_V/a_V) e_\nu (1 + e_\nu)^{-2} - iW(R_W/a_W) e_w (1 + e_w)^{-2} + 4iW_{SF}(R_{WSF}/a_{WSF}) e_{WSF} \times (1 - e_{WSF})(1 + e_{WSF})^{-3} \right]_{\alpha_{22} = \alpha_{42} = 0}. \quad (6)$$

Following Tamura,¹⁵ the potentials are expanded in Legendre polynomials so that

$$V(r, \theta', \phi') = \sum_{\lambda} v_{\lambda}^{(0)}(r) Y'_{\lambda 0} + \alpha_{22} \sum_{\lambda'} v_{\lambda'}^{(2)}(r) Y'_{\lambda' 0} (Y'_{22} + Y'_{2-2}) \\ + \alpha_{42} \sum_{\lambda'} v_{\lambda'}^{(2)}(r) Y'_{\lambda' 0} (Y'_{42} + Y'_{4-2}) \\ + V_{so}(r) + V_{Coul}(r), \quad (7)$$

where

$$v_{\lambda}^{(0)}(r) = 4\pi \int_0^1 d(\cos\theta') Y_{\lambda 0}(\theta') V_1(r, \theta') \quad (8a)$$

and

$$v_{\lambda}^{(2)}(r) = 4\pi \int_0^1 d(\cos\theta') Y_{\lambda 0}(\theta') V_2(r, \theta'). \quad (8b)$$

Reducing the products of spherical harmonics in Eq. (7) yields⁸

$$V(r, \theta', \phi') = \sum_{\lambda} v_{\lambda}^{(0)}(r) Y'_{\lambda 0} + \sum_{\lambda} [\alpha_{22} \tilde{v}_{\lambda}^{(2I)}(r) + \alpha_{42} \tilde{v}_{\lambda}^{(2II)}(r)] \\ \times (Y'_{\lambda 2} + Y'_{\lambda -2}) + V_{so}(r) + V_{Coul}(r), \quad (9)$$

where

$$\tilde{v}_{\lambda}^{(2I)}(r) = \sum_{\lambda'} v_{\lambda'}^{(2)}(r) \left(\frac{5(2\lambda' + 1)}{4\pi(2\lambda + 1)} \right)^{1/2} (20\lambda' 0 | \lambda 0)(22\lambda' 0 | \lambda 2), \quad (10a)$$

and

$$\tilde{v}_{\lambda}^{(2II)}(r) = \sum_{\lambda'} v_{\lambda'}^{(2)}(r) \left(\frac{9(2\lambda' + 1)}{4\pi(2\lambda + 1)} \right)^{1/2} (40\lambda' 0 | \lambda 0)(42\lambda' 0 | \lambda 2). \quad (10b)$$

In Eqs. (10a) and (10b) $(l_1 m_1 l_2 m_2 | l_3 m_3)$ denotes a Clebsch-Gordan coefficient. To express this potential in the space-fixed coordinate system, $Y'_{\lambda \nu}$ is replaced by $\sum_{\mu} D_{\mu\nu}^{\lambda} Y_{\lambda \mu}(\theta, \phi)$, where θ and ϕ are polar angles in the space-fixed coordinate system and $D_{\mu\nu}^{\lambda}$ are the appropriate rotation matrices.²⁰ This yields

$$V(r, \theta, \phi) = \sum_{\lambda \mu} v_{\lambda}^{(0)}(r) D_{\mu 0}^{\lambda} Y_{\lambda \mu}(\theta, \phi) \\ + \sum_{\lambda \mu} [\alpha_{22} \tilde{v}_{\lambda}^{(2I)}(r) + \alpha_{42} \tilde{v}_{\lambda}^{(2II)}(r)] (D_{\mu 2}^{\lambda} + D_{\mu -2}^{\lambda}) \\ \times Y_{\lambda \mu}(\theta, \phi) \\ + V_{so}(r) + V_{Coul}(r). \quad (11)$$

Equation (11) can finally be written as

$$V(r, \theta, \phi) = V_{diag} + V_{couple}, \quad (12)$$

where V_{diag} is the $\lambda = \mu = 0$ part of the first term in Eq. (11) plus $V_{so}(r)$ and $V_{Coul}(r)$, while V_{couple} is the remainder of $V(r, \theta, \phi)$ in Eq. (11).

The wave function of the whole proton-nucleus system is written as¹⁵

$$\Psi = r^{-1} \sum_{J n l_n j_n} R_{J n l_n j_n}(r) \\ \times \sum_{m_j M_n} (j_n m_j j_n M_n | J M) \mathcal{Y}_{l_n j_n m_j} \Phi_{l_n m_n K_n}, \quad (13a)$$

where

$$\mathcal{Y}_{l_j m_j} = \sum_{m_l m_s} (l m_l s m_s | j m_j) i^l Y_{l m_l} \chi_{s m_s}. \quad (13b)$$

The projectile spin state function is $\chi_{s m_s}$ and $\Phi_{l_n m_n K_n}$ represents the target nucleus eigenfunction for the n th excited nuclear state. The target state functions in the rotational model are^{8, 14}

$$\Phi_{I M 0} = \psi_0(\xi) [(2I + 1)/8\pi^2]^{1/2} D_{M 0}^I \quad (14a)$$

and

$$\Phi_{I M 2} = \psi_2(\zeta) [(2I + 1)/16\pi^2]^{1/2} [D_{M 2}^I + (-1)^I D_{M -2}^I] \quad (14b)$$

for the $K^{\pi} = 0^+$ ground band and the $K^{\pi} = 2^+$ γ -vibrational band, respectively. The intrinsic wave functions are denoted in Eqs. (14a) and (14b) by ψ_0 and ψ_2 where ζ denotes the internal nuclear coordinates.

Solving the Schrödinger equation with the potential grouped as in Eq. (12) and the wave function expansion of Eq. (13), yields a set of coupled equations for the functions $R_{J n l_n j_n}(r)$ [see Eq. (25) in Ref. 15]. Evaluating the matrix element for the coupling potential results in (for $K^{\pi} = 0^+$ or 2^+ only),

$$\langle (\mathcal{Y}_U \otimes \Phi_{IK})_{JM} | V_{couple} | (\mathcal{Y}_{I'J'} \otimes \Phi_{I'K'})_{JM} \rangle = \sum_{\lambda} \left(v_{\lambda}^{(0)}(r) \delta_{KK'} (2I' + 1)^{1/2} (I' K \lambda 0 | I K) (1 - \delta_{\lambda 0}) \right. \\ \left. + \delta_{K+K', 2} \sum_{\lambda} v_{\lambda}^{(2)}(r) \sum_{i=1, 2} B^{(i)}(I, I'; \lambda \bar{\lambda}) A(l_j I, l_j' I'; \lambda J S) \right), \quad (15)$$

where

$$B^{(i)}(I, I'; \lambda \bar{\lambda}) = \left(\frac{(2\lambda_i + 1)(2\bar{\lambda} + 1)}{4\pi(2\lambda + 1)} \right)^{1/2} (\lambda_i 0 \bar{\lambda} 0 | \lambda 0)(\lambda_i 2 \bar{\lambda} 0 | \lambda 2) (2I' + 1)^{1/2} (I' 2\lambda - 2 | I 0) \eta_i. \quad (16)$$

The angular momentum factor called $A(ljI, l'j'I')$; $\lambda J S$) is given explicitly by Tamura,¹⁵ and $\lambda_1 = 2$ and $\lambda_2 = 4$, corresponding to the original deformations allowed in Eq. (3). The quantities η_i are given by

$$\eta_1 = \sqrt{2} \langle \psi_0(\xi) | \alpha_{22} | \psi_2(\xi) \rangle \quad (17a)$$

and

$$\eta_2 = \sqrt{2} \langle \psi_0(\xi) | \alpha_{42} | \psi_2(\xi) \rangle. \quad (17b)$$

The expression in Eq. (17a) becomes, following Bohr¹⁴ and Tamura,⁸

$$\begin{aligned} \eta_1 &= \sqrt{2} \langle \psi_0(\xi) | (\beta/\sqrt{2}) \sin\gamma | \psi_2(\xi) \rangle \\ &\approx \langle \psi_0(\xi) | \beta\gamma | \psi_2(\xi) \rangle, \end{aligned} \quad (18)$$

$$\eta_1 \approx \beta\gamma_0.$$

In fitting the inelastic angular distribution data corresponding to the excitation of states in the γ -vibrational band, the matrix elements η_1 and η_2 are varied to produce the best overall agreement in magnitude of the calculations with the data for both the 2_2^+ , 4.24 MeV and the 4_2^+ , 6.01 MeV states.

The coupled-channels code JUPITER²¹ was modified to include this additional $\alpha_{42}(Y'_{42} + Y'_{4-2})$ vibrational multipole term as in Eq. (15), as well as relativistic kinematics²² needed in the calculations for the 800 MeV proton scattering data.

III. CALCULATIONS AND RESULTS

In an investigation of the effect of the additional $\alpha_{42}(Y'_{42} + Y'_{4-2})$ vibrational mode, the values of the parameters α_{20} , α_{40} , η_1 , and η_2 were varied freely to obtain the best description of the 800 MeV (p, p') cross sections for the states of the ground state rotational band and of the γ -vibrational band. These *same* intrinsic deformations and vibrational mode strengths were then used in corresponding coupled-channels calculations for the 20.3 and 40 MeV (p, p') data. Appropriate phenomenological^{15,18} optical potential parameters were selected from the literature, specifically Refs. 2, 6, and 7 for 800, 40, and 20.3 MeV incident proton energies, respectively. For quick reference, these parameters are also given in Table I.

At 800 MeV it has previously been shown, for the low lying natural parity states in a variety of nuclei, that essentially equivalent predictions of the inelastic angular distributions result whether spin-orbit terms are fully omitted or fully included, provided equivalent fits to the elastic angular distributions have been obtained.²³ By full inclusion of the spin-orbit term, we mean inclusion of spin-orbit effects in *both* the diagonal and off-diagonal parts of Eq. (12), or in other words, a deformed spin-orbit potential is to be used.²³ Such deformed spin-orbit potentials are required in order to get a satisfactory description of inelastic analyzing power data at 800 MeV.^{23,24} Thus, when only angular distributions are to be described, omission of the spin-orbit effects altogether is desirable, since the coupled-channels calculations are tremendously speeded up and numerically simplified. At lower energies, say 25 to 50 MeV, the effect of a deformed spin-orbit potential on the inelastic angular distributions is, however, less important, so that it becomes permissible to omit spin dependence in the off-diagonal portion of the potential while retaining it in the diagonal portion. Since good fits cannot be obtained to the 20.3 and 40 MeV elastic data of the quality shown in Refs. 6 and 7, if spherical spin-orbit potentials are not included, these diagonal terms will be taken into account in the lower energy calculations. At 800 MeV, however, all spin effects will be entirely omitted.

At each of the three energies, two distinct types of calculations were performed. The first had $\eta_2 = 0$, while $R\eta_1$ was adjusted to produce the best overall agreement with the magnitude of the cross section for population of the 4.24 MeV 2_2^+ state at 800 MeV, and the same value of $R\eta_1$ was then used for the 20.3 and 40 MeV calculations. The results of these coupled-channels calculations are indicated by the dashed curves in Figs. 1-3. As no direct path is allowed between the ground state of ²⁴Mg and the 4_2^+ member of the γ -vibrational band, one sees the usual^{2-8,10} discrepancies in magnitude and shape between the predictions and data for the γ -band members.

TABLE I. The optical potential parameters of Refs. 2, 6, and 7 used in the coupled-channels calculations as reported here in the notation of Eqs. (1)-(3) of the text and of Ref. 15. The radii r_i are equal to $R_i A^{-1/3}$ where $i = V, W$, or WSF . All potential strengths are in MeV and each radius and diffuseness is in fermis.

Energy (MeV)	V	r_V	a_V	W	r_W	a_W	W_{SF}	r_{WSF}	a_{WSF}	V_{so}	r_{so}	a_{so}	r_c
20.3	48.62	1.15	0.67	0.0	7.76	1.37	0.28	4.56	0.94	0.40	1.20
40.0	38.61	1.22	0.65	10.62	1.26	0.67	0.02	1.26	0.67	6.2	1.01	0.75	1.20
800.0	-5.3	0.929	0.45	100.0	0.929	0.545	16.0	0.446	0.397	0.0	1.05

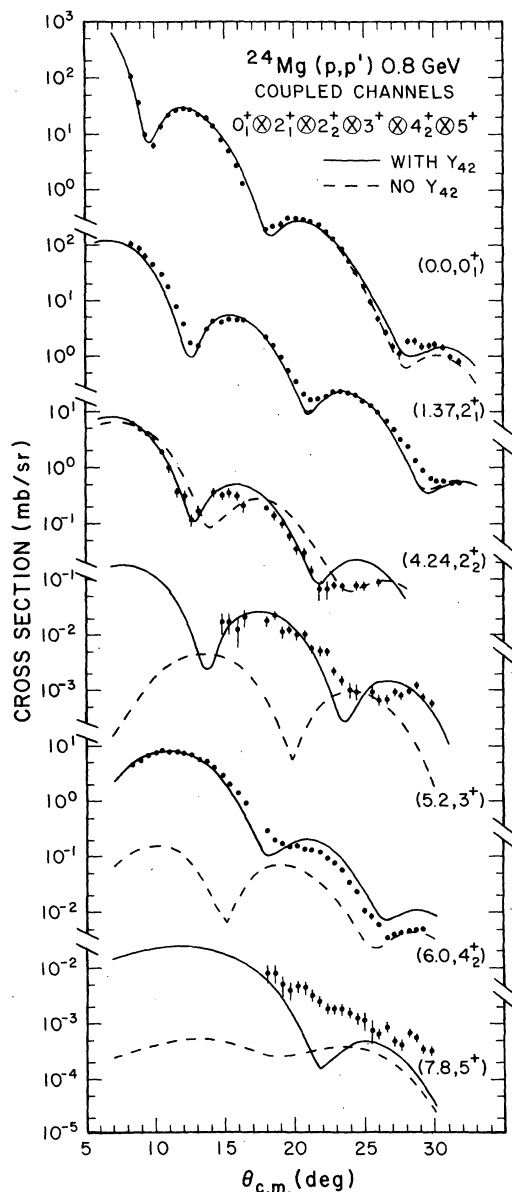


FIG. 1. Proton inelastic scattering from ^{24}Mg at 800 MeV incident energy. The data are from Ref. 2. Coupled-channels calculations, in which each of the six states for which data are shown are included in the coupling scheme, are represented by the dashed curves ($\eta_2=0$) and the solid curves ($\eta_2 \neq 0$). The significant improvement for nonzero η_2 is an indication of the importance of a direct transition from the ground state to the 4_2^+ member of the γ -vibrational band, as discussed in detail in the text.

In the second series of calculations, $R\eta_1$ and $R\eta_2$ were adjusted freely to produce the best overall description of the 800 MeV data for the 4.24 MeV 2_2^+ and 6.01 MeV 4_2^+ states of the γ band.

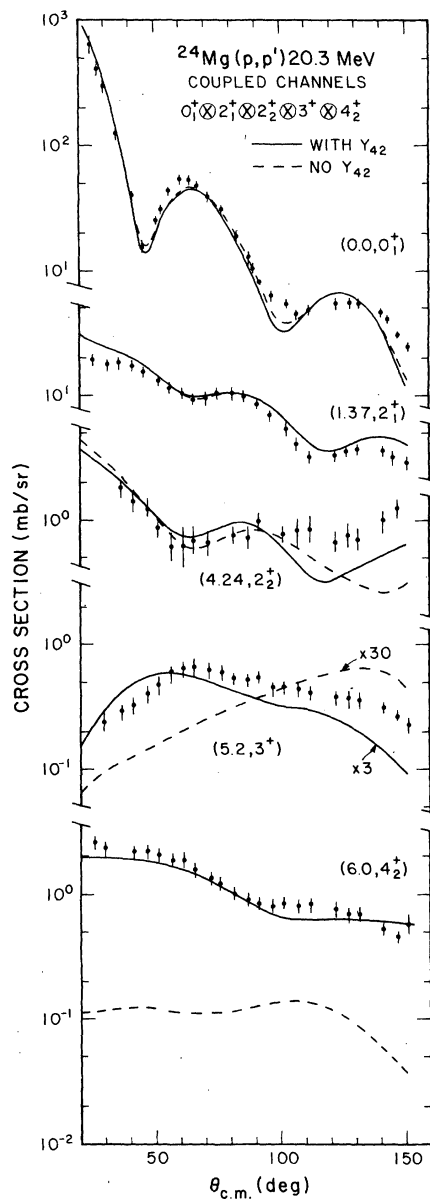


FIG. 2. Same as Fig. 1, except for an incident energy of 20.3 MeV. The data are from Ref. 7. Since no data are available for the 5^+ state at this incident proton energy, it is omitted from the coupling scheme. For the 3^+ state, in this figure only, scale factors ($\times 30$ for $\eta_2=0$, $\times 3$ for $\eta_2 \neq 0$) have been used to position the predictions relative to the data.

Once again, these same values were used for the 20.3 and 40 MeV calculations; the results are displayed as the solid curves in Figs. 1-3. It should be appreciated that in each calculation *all* states for which data are displayed are coupled to one another.

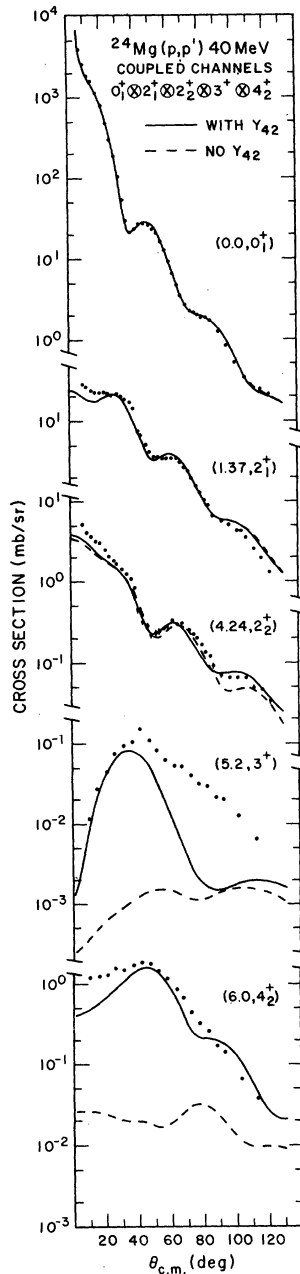


FIG. 3. Same as Fig. 1, except for an incident proton energy of 40 MeV. The data are from Ref. 6.

The coupled-channels analysis of Blanpied *et al.*,² which did not include $\Delta l = 4$ transitions to the γ band, obtained deformation lengths which reproduced the 800 MeV data for the 0_1^+ ground state, and the 2_1^+ , 1.37 MeV and 4_1^+ , 4.12 MeV members of the ground state rotational band. These lengths, in our notation, are $R\alpha_{20} = 1.61$ fm and $R\alpha_{40} = -0.05$ fm. As Figs. 1–3 indicate, these deformation lengths, which were used in all our calcu-

lations, provide excellent descriptions of the ground and 2_1^+ , 1.37 MeV states' angular distributions, independent of the assumed value for η_1 and η_2 (compare the dashed and solid curves).

Turning to the analysis of the 800 MeV data with $\eta_2 = 0$, we find that the value of $R\eta_1$ which best describes the 2_2^+ , 4.24 MeV state's angular distribution is $R\eta_1 = 0.56$ fm, but the "best" is not very good, and for the other members of the band, the results are completely inadequate. It is seen that the prediction for the 2_2^+ angular distribution is out of phase with the data by from 1 to 2 degrees, although agreeing in magnitude, while for the 5.2 MeV 3^+ , the 4_2^+ at 6.01 MeV, and the 7.8 MeV 5^+ , the predicted magnitudes are too low by factors of 10 to 100, and the predicted shapes are quite wrong.

On the other hand, the analysis with $R\eta_1 = 0.43$ fm and $R\eta_2 = 0.72$ fm, with results indicated by the solid curves in Figs. 1–3, gives a reproduction of the 800 MeV data that is overall excellent, comparatively speaking. Of course, the inclusion of the $\alpha_{42}(Y'_{42} + Y'_{4-2})$ term in Eq. (3) would be expected to improve the fit to the 4_2^+ , 6.01 MeV state's angular distribution. But as an impressive by-product, we find that the predicted angular distribution for the 2_2^+ , 4.24 MeV state is shifted nicely into phase with the data, and the prediction for the angular distribution of the 3^+ , 5.2 MeV state is also dramatically altered in shape and magnitude, bringing it too into good agreement with experiment. Even for the 5^+ , 7.8 MeV state there is considerable improvement in the discrepancy between data and the coupled-channels prediction.

It should be mentioned that simple DWBA calculations for the 4_2^+ inelastic cross section² become gradually out of phase with the data at angles greater than 25° , whereas the present coupled-channels calculations with $\eta_2 \neq 0$ remain in phase with the data over the full experimental angular range (8° – 29°). In this comparison one can see that the effect of the multistep paths to the 4_2^+ state are somewhat more subtle than one might naively expect in ^{24}Mg .

The description of the γ -vibrational band, while vastly improved, is not perfect. The 800 MeV calculations with η_2 nonzero slightly overestimate the magnitudes of the 2_2^+ and 4_2^+ states at the larger angles, predict too deep a minimum near 24° for the 3^+ state, and continue to fail to reproduce the angular distribution of the 5^+ state. As these discrepancies are rather small compared to the original discrepancy removed by the inclusion of the $\alpha_{42}(Y'_{42} + Y'_{4-2})$ terms, they could well result from a complex interplay between several less important processes omitted in the present calculations. These include additional terms of the

$\alpha_{\lambda_2}(Y'_{\lambda_2} + Y'_{\lambda_2-2})$ form, spin-flip processes, couplings to other bands, or even inadequacies of the simple macroscopic collective rotational model.

Calculations were also performed at 800 MeV with the relative algebraic sign of $R\eta_1$ and $R\eta_2$ reversed, so that $R\eta_2 = -0.72$ fm while $R\eta_1 = 0.43$ fm as before. The prediction for the 4_2^+ state is not affected too seriously; however, the prediction for the 2_2^+ state at 4.24 MeV is shifted completely out of phase with the experimental data, producing far worse agreement than that shown for the dashed curve in Fig. 1. A calculation coupling in the 4_1^+ state at 4.12 MeV was also performed, using the values of $R\alpha_{20}$, $R\alpha_{40}$, $R\eta_1$, and $R\eta_2$ which produced the solid curves in Fig. 1. This gives a description of the 4_1^+ state which reproduces the experimental data and the $\eta_2 = 0$, coupled-channels calculation (both shown in Ref. 2) quite well and does not change the predictions for the γ -vibrational band in any significant way. The 4_1^+ state is thus omitted from the figures.

Using these established values of $R\alpha_{20}$, $R\alpha_{40}$, $R\eta_1$, and $R\eta_2$, we then repeated coupled-channels calculations for $^{24}\text{Mg}(p, p')$ at 20.3 and 40 MeV, with the results shown by the solid lines in Figs. 2 and 3. The results are very similar to those found at 800 MeV; the fit to the 2_2^+ , 4.24 MeV state is improved at larger angles, the fit to the 4_2^+ , 6.01 MeV state is excellent as expected, and there is a dramatic improvement in the predicted shape and magnitude of the angular distribution for the 3^+ state at 5.2 MeV. Since at least a major part of the remaining discrepancy for the 3^+ angular distribution at each of the three energies can be ascribed to spin-flip processes, the reduced importance of spin flip in the population of this state in ^{24}Mg with increasing proton energy is qualitatively demonstrated by a study of Figs. 1-3. The overall factor of 3 discrepancy in magnitude at 20.3 MeV is essentially eliminated by 40 MeV, at least at the forward angles, while the fit to the angular distribution at 800 MeV is reasonably acceptable.

IV. CONCLUSIONS

The principal results of our analysis may be summarized as follows:

- (1) The $\alpha_{42}(Y'_{42} + Y'_{4-2})$ vibrations are of extreme importance in accounting for the strength and details of the inelastic proton scattering to the γ -vibrational band of ^{24}Mg . A rather large value of $R\eta_2 = 0.72$ fm was obtained as a quantitative measure of the strength of this type of transition.
- (2) The value of $R\eta_1$ inferred from previous analyses² is found to be significantly reduced from 0.56 to 0.43 fm, a decrease of 23%.
- (3) The same intrinsic deformation and vibration lengths, $R\alpha_{20}$, $R\alpha_{40}$, $R\eta_1$, and $R\eta_2$, provide a relatively satisfactory description of the (p, p') data for the 2_1^+ , 1.37 MeV, the 2_2^+ , 4.24 MeV, and the 4_2^+ , 6.01 MeV states in ^{24}Mg at incident energies varying from 20 to 800 MeV. Tolerably good fits are also obtained at all energies for the 3^+ , 5.2 MeV state, from which one can qualitatively estimate the importance of spin-flip contributions to the inelastic cross section for that state to be a diminishing function of incident proton energy, and quite small at 800 MeV.

It is clear that the $\alpha_{42}(Y'_{42} + Y'_{4-2})$ vibrational mode should always be included in coupled-channels analyses of inelastic scattering data for the γ -vibrational bands of deformed nuclei. This additional vibrational mode should be included in the description of the inelastic scattering of α particles as well as other projectiles to states in the γ -vibrational bands of deformed nuclei. A worthwhile application of this type of calculation would be to the recent 1.37 GeV α inelastic scattering data from ^{24}Mg .²⁵

Note added in proof: After completing this work an unpublished thesis by M. Reed was found in which a coupling scheme similar to that used here was successfully applied to α inelastic scattering. The reference is M. Reed, UCRL 18414 (1968).

This research was supported in part by the United States Department of Energy.

¹J. D. Rogers, *Annu. Rev. Nucl. Sci.* **15**, 241 (1965);

R. K. Sheline, *Rev. Mod. Phys.* **32**, 1 (1960); J. P. Davidson, *ibid.* **37**, 105 (1965).

²G. Blanpied *et al.*, *Phys. Rev. C* **20**, 1490 (1979), this issue.

³A. A. Rush and N. K. Ganguly, *Nucl. Phys.* **A117**, 101 (1968).

⁴J. Eenmaa, R. K. Cole, C. N. Waddell, H. S. Sandhu, and R. R. Dittman, *Nucl. Phys.* **A218**, 125 (1974).

⁵I. Lovas, M. Rogge, U. Schwinn, P. Turek, and D. Ingham, *Nucl. Phys.* **A286**, 12 (1977).

⁶B. Zwieglinski, G. M. Crawley, H. Nann, and J. A. No-

len, Jr., *Phys. Rev. C* **17**, 872 (1978); B. Zwieglinski, G. M. Crawley, W. Chung, H. Nann, and J. A. Nolen, Jr., *ibid.* **18**, 1228 (1978).

⁷R. M. Lombard, J. L. Escudie, and M. Soyeur, *Phys. Rev. C* **18**, 42 (1978).

⁸T. Tamura, *Nucl. Phys.* **73**, 241 (1965).

⁹J. Kokame, K. Fukunaga, N. Inoue, and H. Nakamura, *Phys. Lett.* **8**, 342 (1964).

¹⁰J. S. Vincent, E. T. Boschitz, and J. R. Priest, *Phys. Lett.* **25B**, 81 (1967).

¹¹I. M. Naqib and J. S. Blair, *Phys. Rev.* **165**, 1250 (1968).

- ¹²M. K. Pal and A. P. Stamp, *Phys. Rev.* 158, 924 (1967).
- ¹³H. P. Morsch, D. Dehnhard, and T. K. Li, *Phys. Rev. Lett.* 34, 1527 (1975).
- ¹⁴A. Bohr, *Mat. Fys. Medd. Dan. Vid. Selsk.* 26, No. 14 (1952); A. Bohr and B. R. Mottelson, *Nuclear Structure* (Benjamin, Reading, Mass., 1975), Vol. II.
- ¹⁵T. Tamura, *Rev. Mod. Phys.* 37, 679 (1965); *Annu. Rev. Nucl. Sci.* 19, 99 (1969).
- ¹⁶P. M. Endt and C. Van der Leun, *Nucl. Phys.* A310, 1 (1978).
- ¹⁷G. R. Satchler, *Nucl. Phys.* 55, 1 (1964).
- ¹⁸C. M. Perey and F. G. Perey, *At. Data Nucl. Data Tables* 13, 293 (1974).
- ¹⁹B. J. Verhaar, in *Lecture Notes in Physics, Polarization Nuclear Physics*, edited by J. Ehlers (Springer, Berlin, 1974), p. 268 and references therein.
- ²⁰D. M. Brink and G. R. Satchler, *Angular Momentum* (Oxford University, London, 1962).
- ²¹T. Tamura, Oak Ridge National Laboratory Report No. ORNL-4152, 1967.
- ²²W. R. Coker, L. Ray, and G. W. Hoffmann, *Phys. Lett.* 64B, 403 (1976).
- ²³L. Ray and W. R. Coker, *Phys. Lett.* 79B, 182 (1978).
- ²⁴R. P. Liljestrang *et al.*, *Phys. Rev. Lett.* 42, 363 (1979).
- ²⁵T. S. Bauer *et al.*, *Phys. Rev. C* 19, 1438 (1979).